EARTH SURFACE PROCESSES AND LANDFORMS
Earth Surf. Process. Landforms **35**, 1240–1246 (2010)

Published online 4 June 2010 in Wiley InterScience
(www.interscience.wiley.com) DOI: 10.1002/esp.2020

ESEX Commentary

Examining the physical components of boundary shear stress for water-worked gravel deposits

James R. Cooper* and Simon J. Tait
School of Engineering, Design and Technology, University of Bradford, Bradford, BD7 1DP, UK

Received 16 November 2009; Revised 22 February 2010; Accepted 2 March 2010

*Correspondence to: J. R. Cooper, School of Engineering, Design and Technology, University of Bradford, Richmond Road, Bradford, BD7 1DP, UK. E-mail: j.cooper2@bradford.ac.uk

ESPL
Earth Surface Processes and Landforms

ABSTRACT: It is argued in this commentary that, in order to understand better the physical mechanisms that generate boundary shear stress over water-worked gravel beds, flow velocity data should be re-evaluated by spatial averaging the Reynolds equations to produce time- and space-averaged (double-averaged) momentum equations. A series of laboratory experiments were conducted in which the flow velocities were measured using a PIV system over two water-worked gravel deposits. Combined with detailed data on the bed surface topography and vertical porosity, the physical components of shear stress were obtained. This enabled the various momentum transfer mechanisms present above, within and at the interface of a porous, fluvial deposit, to be quantified. This included the examination of the relevant contributions of temporal and spatial fluctuations in velocity and surface drag to the overall momentum transfer. It is demonstrated that double-averaging represents a logical framework for assessing the fluid forces responsible for sediment entrainment and for investigating intragravel flow and sediment–water interface exchange mechanisms within the roughness layer in water-worked gravel deposits. By considering the physical components of shear stress and their relative sizes it was possible to provide a physically based explanation for existing observations of enhanced mobility of gravel–sand mixtures and the transfer of solutes into porous, gravel deposits. This analysis reveals the importance of obtaining co-located, high quality spatial data on the flow field and bed surface topography in order to gain a physical understanding of the mechanisms which generate boundary shear stress. Copyright © 2010 John Wiley & Sons, Ltd.

KEYWORDS: boundary shear stress; fluid forces; water-worked gravel beds; PIV; double-averaging

Introduction

Boundary shear stress is a measure of the average momentum absorbed by a boundary from a moving fluid. It dictates the momentum available from the fluid to entrain, transport and deposit material at the fluid–boundary interface. It is one of the most widely used terms in process geomorphology, and its evaluation is of great interest when studying flows over fluvial sediment deposits. In this commentary we argue that the existing approaches used to evaluate boundary shear stress can be improved in order to provide additional physical insight. We demonstrate, using laboratory data, an approach which involves describing boundary shear stress through time and space averaging of the Navier–Stokes equations. We show that this provides a consistent way to relate spatially-averaged flow and boundary roughness properties with boundary shear stress on a water-worked gravel surface. It offers an improved way of investigating the impact of near-bed flows on sediment entrainment, intragravel flow and sediment–water interface exchange processes. Although this approach uses concepts that are well developed in the fields of porous media, atmospherics, and most recently in hydraulic engineering, it has never been exploited within geomorphology. The aim of this commentary is to introduce this approach and to demonstrate briefly its strength for examining momentum fluxes over porous, water-worked sediment deposits.

Turbulent flow has been classically viewed as statistically random. This led to the expectation that turbulence could be clarified experimentally by performing single point velocity measurements, and describing the collected data by means of conventional statistical tools. It is now well established that turbulent flows over gravel beds are far from random, and exhibit coherence in time and space (Lamarre and Roy, 2005; Cooper and Tait, 2008; Hardy *et al.*, 2009). For example, several studies have reported on the existence of vortically-based, large, depth-scale flow structures (Shvidchenko and Pender, 2001; Roy *et al.*, 2004).

Despite this evidence of spatial coherence, the traditional approach to studying flows over rough boundaries has been based on the time-averaged Navier–Stokes equations, known

more commonly as the Reynolds equations. Using this approach, the products of the fluctuating velocity deviations from their time-averaged values give rise to a turbulent stress term, the Reynolds stress $-\overline{u'w'}$ and a viscous term $\nu[d\bar{u}/dz]$. With an assumption of 2-D, steady, uniform flow it follows that the total fluid shear stress at an elevation z can be obtained. The boundary shear stress at a single location at the roughness crest elevation z_c can be estimated by

$$\tau_0(z_c) = \rho g S_b(z_w - z_c) = \rho\left[-\overline{u'w'} + \nu\frac{\partial\bar{u}}{\partial z}\right]_{z=z_c} \quad (1)$$

where ρ is fluid density, g is gravitational acceleration, S_b is the average boundary slope, z_w is the elevation of the water surface, ν is kinematic viscosity, u and w is instantaneous streamwise and vertical velocity, $u' = u - \bar{u}$, $w' = w - \bar{w}$, and $\bar{u}$ and $\bar{w}$ is time-averaged streamwise and vertical velocity. This approach has a number of consequences when examining turbulent flows over rough sediment deposits:

(1) The Reynolds approach assumes no flow spatial variability in the streamwise and lateral direction, so it can only define explicitly boundary shear stress for a single point on the boundary. This might be an appropriate assumption for a boundary with no topographical variation, but clearly this assumption is not suitable for sediment boundaries with complex geometry.
(2) Momentum exchange between a water-worked sediment boundary and a fluid occurs progressively with the vertical variation in bed surface elevation, rather than suddenly across a single plane at a single vertical position. This makes the shear stress experienced by parts of the boundary different from the total fluid shear stress at the roughness crest, as described by the Reynolds equations. This difference is negligible for rough boundary flows with high relative submergence, but becomes significant when the ratio between flow depth and roughness size is low.
(3) At low relative submergences there is significant retardation in Reynolds stress, relative to an assumed vertical linear distribution, close to and within the roughness elements (Nikora and Goring, 2000; Campbell *et al.*, 2005). The region in which the retardation occurs in Reynolds stress is said to indicate the existence of a zone where the flow is spatially variable. This variability indicates that additional mechanisms for momentum extraction must emerge within this zone to balance the overall momentum between the fluid and the sediment boundary. These additional mechanisms are not described by the Reynolds equations.

Data Collection and Analysis

We argue that, in order to understand the physical mechanisms that generate boundary shear stress, flow velocity data should be re-evaluated by spatial averaging the Reynolds equations to produce time- and space-averaged (double-averaged) momentum equations. By spatial area averaging (in a plane parallel to the bed) and using a spatial decomposition, the spatial variability in the flow in the streamwise and lateral direction, and the associated physical mechanisms, can be taken into account. This approach will be demonstrated using data from a series of laboratory experiments in which the flow velocities were measured using a PIV system over two water-worked gravel deposits, where detailed data on the bed surface topography and vertical porosity had first been obtained. Flow velocity time series, each containing 3000 instantaneous streamwise and vertical velocity measurements, were obtained through the flow depth at 549 planar locations over the deposits. This was achieved by taking vertical plane measurements at nine lateral locations for a sampling time of 330 s and at a rate of 9 Hz. The separation distance between measurements in a single plane was 2·25 mm. The bed surface topography was measured with a laser displacement sensor positioned on an automated traverse. The flow velocity data was combined with the detailed topography data to identify and estimate the components of shear stress.

Table I. Summary of the grain size, surface and subsurface properties of the two deposits, where D_{50} and D_{84} are the grain sizes at which 50 and 84% of the bed material is finer, respectively, σ_D is the sorting coefficient, σ_b is the standard deviation of bed surface elevations z_b, k is the range of z_b, H_x and H_y are the Hurst exponents for the streamwise and lateral variations in z_b, respectively, ϕ_{sub} is the mean bulk subsurface porosity and K is the hydraulic conductivity. More details can be found in Cooper and Tait (2009)

Property	Unimodal deposit	Bimodal deposit
D_{50} (m)	0·00497	0·00442
D_{84} (m)	0·00700	0·00659
$D_{\tilde{x}}$ (m)	0·00495	0·00380
σ_D (m)	0·00140	0·00190
σ_b (m)	0·00214	0·00170
k (m)	0·0152	0·0137
H_x (m)	0·452	0·463
H_y (m)	0·320	0·368
ϕ_{sub} (%)	17·5	12·0
K (m s^{-1})	$1{\cdot}00 \times 10^{-4}$	$4{\cdot}07 \times 10^{-5}$

Each deposit was formed by feeding in a sediment mixture at the upstream end of the flume at twice the transport capacity of the flow, in order to form a water-worked deposit. Two different mixtures were used: a log-normal, unimodal grain-size distribution and a slightly bimodal grain-size distribution (Table I). The former consisted of 100% gravel with 0·15 mm $< D <$ 14 mm and a median grain diameter D_{50} of 4·97 mm. The bimodal mixture contained 75% of the same gravel and 25% sand to produce a mixture with the same range of grain-sizes and D_{50} of 4·41 mm. The two mixtures were designed to produce similar values of D_{50}, so that the average scale of the grains in each of the deposits were comparable. This resulted in the formation of two water-worked sediment deposits with different surface geometries and subsurface properties (Table I and Figure 1). This made it possible to investigate the influence of sand and porosity on the relative role of different momentum transfer mechanisms. For each deposit, six tests were carried out at a single bed slope using a range of relative submergences (Table II). The selected flow conditions were below those required for bed movement, so the bed surface topography did not change during each test. The experimental programme was designed so that tests with similar values of relative submergence and bed slope were conducted for each deposit, enabling the results to be compared directly between the two sediment deposits. More details on the experimental approach is given in Cooper (2006).

The velocity data was examined using an approach, described by Nikora *et al.* (2007), which involves decomposing the time-averaged variables into spatially-averaged (denoted by angle brackets) and spatially fluctuating (denoted by a wavy overbar) components, such that $\bar{u}_i = \langle\bar{u}_i\rangle + \tilde{u}_i$, where u_i is the instantaneous velocity in the ith direction. The spatial fluctuations in velocity arise from the difference between the double-averaged $\langle\bar{u}_i\rangle$ and time-averaged $\bar{u}_i$ values, $\tilde{u}_i = \bar{u}_i - \langle\bar{u}_i\rangle$,

similar to the conventional Reynolds decomposition. This produces information offering better physical insight into the mechanisms that contribute to the overall transfer of momentum at a vertical location in the flow. By averaging over a spatial domain, the decomposition can be used to assess all the forces on a rough, sediment boundary under an averaging area A_0. In our paper the area is equal to 143 × 9 mm^2 (streamwise×lateral), which is the planar area covered by the PIV measurements. The streamwise length is given by the length of the PIV image and the lateral dimension is the total lateral span covered by the nine PIV planes (the light sheet thickness was ~1 mm). Following the work of Nikora *et al*. (2007), for a 2-D, steady, uniform flow over a static boundary with a variable vertical porosity, the total force F_b on the boundary under A_0 can be defined as

$$F_b(z_t) = \rho g S_b A_0 (z_w - z_c) + \int_{z_t}^{z_c} \phi A_0 \rho g S_b (z_c - z)\, dz$$
$$= \rho \phi A_0 \left[-\langle \overline{u'w'} \rangle - \langle \tilde{u}\tilde{w} \rangle + \nu \frac{\partial \langle \bar{u} \rangle}{\partial z} \right]_{z=z_t} + \int_{z_t}^{z_c} (F_{fd} + F_{vd})\, dz \quad (2)$$

where

$$F_{fd} = \int_S \bar{p} n_x dS \quad (3)$$

$$F_{vd} = \int_S \nu \left[\frac{\partial \bar{u}}{\partial x} n_x + \frac{\partial \bar{u}}{\partial y} n_y + \frac{\partial \bar{u}}{\partial z} n_z \right] dS \quad (4)$$

In these equations F_{fd} and F_{vd} are the form drag and viscous drag, p is fluid pressure and $\mathbf{n} = \{n_x, n_y, n_z\}$ is the unit vector normal to the surface S of the section of bed described by the area A_0. An important parameter in Equation (2) is the roughness geometry function ϕ, which is defined as A_f/A_0, where A_f is the area of water in the averaging domain at z and A_0 is the area at z_c. This function is a measure of the variation in the geometrical properties of the water-worked boundary. It accounts for the spatial properties of the boundary in all three dimensions. It enables the influence of the surface geometry on the momentum equation to be extended into the roughness elements down to the roughness trough, which is not possible with the Reynolds equations. Figure 1 shows how the measured value of ϕ (derived from the laser bed scans) changes within the surface of the two deposits and reveals the vertical variation in the fluid proportion within the gravel and gravel–sand deposit. The dependency of F_b (and therefore boundary shear stress) on ϕ in Equation (2) means that the double-averaging approach provides a consistent way to link the spatially-averaged boundary shear stress to the vertical variations in the bed surface geometry.

This approach offers the capability to examine the vertical variation in the different components of the overall force at

Table II. Summary of the experimental conditions, where U denotes the unimodal deposit, B denotes the bimodal deposit, S_b is the bed slope, Q is the flow discharge, d is the flow depth and k is the geometric roughness height

Run	S_b	Q (m^3 s^{-1})	d (m)	d/k
1U	0·00285	0·00159	0·0181	1·2
2U	0·00285	0·00389	0·0286	1·9
3U	0·00285	0·00635	0·0395	2·6
4U	0·00285	0·00869	0·0484	3·2
5U	0·00285	0·0140	0·0628	4·1
6U	0·00285	0·0280	0·0900	5·9
1B	0·00284	0·00143	0·0173	1·3
2B	0·00284	0·00276	0·0272	2·0
3B	0·00284	0·00527	0·0373	2·7
4B	0·00284	0·00809	0·0455	3·3
5B	0·00284	0·0127	0·0595	4·3
6B	0·00284	0·0245	0·0845	6·2

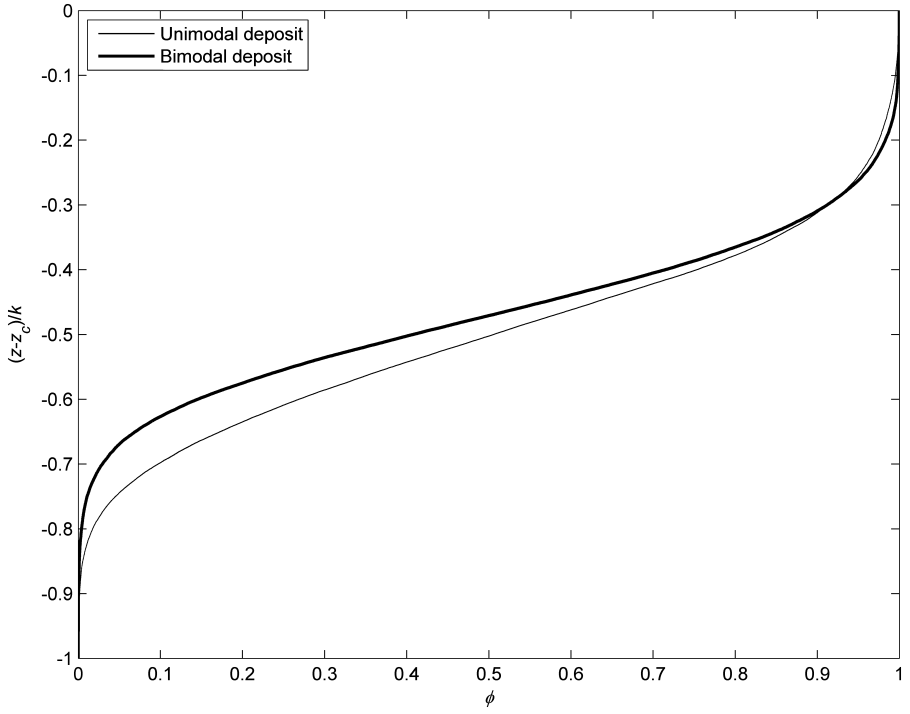

Figure 1. Vertical change in the roughness geometry function (porosity) ϕ for the surfaces of the two water-worked gravel deposits.

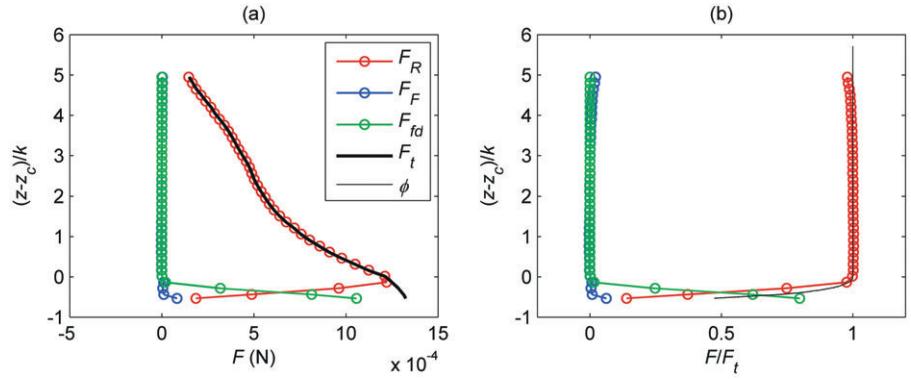

Figure 2. Vertical distribution of force components over a defined plan area A_0 for run 6U, where F_R and F_F are the fluid forces caused by Reynolds and form-induced stress, respectively, F_{fd} is form drag and F_t is the total fluid force. This figure is available in colour online at www.interscience.wiley.com/journal/espl

the boundary. For the turbulent flow field above the roughness layer, where $-\langle\tilde{u}\tilde{w}\rangle$, F_{fd} and $F_{vd} = 0$ and $\phi = 1$, Equation (2) is equivalent to that derived from the Reynolds equations. However within the roughness layer, the spatial averaging procedure introduces additional terms to those which appear in the Reynolds equations. The Reynolds stress is now spatially averaged, so any spatial variability in this stress is taken into account. The total fluid force is also composed of the force contributed by form-induced stress $\langle\tilde{u}\tilde{w}\rangle$, which is the streamwise averaged momentum flux that arises due to spatial heterogeneity in the time-averaged flow. The other additional terms are the form drag and viscous drag, which appear due to pressure and viscous forces on the surface of the sediment boundary.

Experimentally, for the 2D, fully turbulent, steady, uniform flows studied over the two water-gravel deposits, the total fluid force F_t at level z within the surface grains can be approximated by

$$F_t(z) = -\rho\phi A_0\left[\langle\overline{u'w'}\rangle(z) + \langle\tilde{u}\tilde{w}\rangle(z)\right] + \int_z^{z_c} 0.5C_D\rho\langle\bar{u}\rangle^2(z)A_e(z)dz \quad (5)$$

where C_D is the drag coefficient and A_e is the exposed frontal area of the sediment grains (resolved from laser scans of the bed surface topography). Two viscous terms are omitted from Equation (2) because the viscous stress term is assumed to be negligible. The fluid forces caused by Reynolds stress $F_R(z)$ are given by $-\rho\phi A_0\langle\overline{u'w'}\rangle(z)$ and those by form-induced stress $F_F(z)$ are equal to $-\rho\phi A_0\langle\tilde{u}\tilde{w}\rangle(z)$. Form drag $F_{fd}(z)$ is estimated through $\int_z^{z_c} 0.5C_D\rho\langle\bar{u}\rangle^2(z)A_e(z)dz$. Within the roughness elements, F_t at level z is equal to the force contributed by the weight of the water above $\rho g S_b A_0 (z_w - z_c) + \phi A_0\rho g S_b (z_c - z)$. With knowledge of $\langle\overline{u'w'}\rangle$ and $\langle\tilde{u}\tilde{w}\rangle$ it is possible to estimate a value of C_D at each of the measured planes which maintains overall momentum balance within the roughness layer (i.e. set C_D at each z so that F_t from Equation (5) is equal to this weight force). The C_D values were found to fall within the experimental range of Schmeeckle *et al.* (2007) and as such appear reasonable. Equation (5) reveals that only by obtaining co-located, high quality spatial data on the flow field and bed surface topography is it possible to quantify the various momentum transfer mechanisms present above, within and at the interface of a porous water-worked sediment deposit.

Contributions to the Total Fluid Force

To describe the importance of the various terms and how Equation (2) can be used to examine the relative importance of the different momentum transfer mechanisms, an example is given in Figure 2 of the vertical distribution of the force components in Equation (5). The total force supplied by the fluid over a defined plan area A_0 between z_w and z_c is almost totally balanced by the Reynolds stress in the fluid (Figure 2b). This represents the force which is transferred from the flow above the bed and into the flow and bed elements within the roughness layer. This is almost entirely due to turbulent fluid exchange. At a very small distance above the roughness crest, reduction in the Reynolds stress begins to occur (Figure 2a). This is where persistent vortices behind roughness elements cause a small additional force to be transferred towards the roughness trough caused by form-induced stress. It also represents the upper effective boundary of the roughness layer, where the flow has significant spatial heterogeneity. Here, force is transferred from the flow above by both turbulence and spatial heterogeneity in the time-averaged flow. At the upper height of the roughness layer, the total fluid force is a reflection of the total momentum exchange between the roughness layer and the overlying flow.

Within the roughness elements at a level z, there is an additional force of $\rho g S_b\phi A_0 (z_c - z)$ caused by the weight of the fluid in the roughness layer causing the total force to increase. The additional force is balanced by surface form drag and fluid forces caused by temporal and spatial velocity variation. This introduces a major change to the mechanisms of momentum exchange. Total force $\rho g S_b A_0[(z_w - z_c) + \phi(z_c - z)]$ at z is thus partly transferred further down by turbulent exchange and spatial heterogeneity in the time-averaged flow, and partly extracted by form drag with the bed surface. Within this region, the vertical variation of the force contributed by Reynolds and form-induced stress and form drag closely resembles the change in ϕ and is therefore controlled by the geometry of the deposit.

An examination of how the relative contributions of the force components within the roughness layer change with relative submergence reveals some important consequences for sediment–water interface exchange processes (Figure 3). The most interesting is that the contributions from flow turbulence rise as relative submergence increases. Studies have shown that the exchange of solutes between the overlying flow and the near stream region of a river bed is caused by

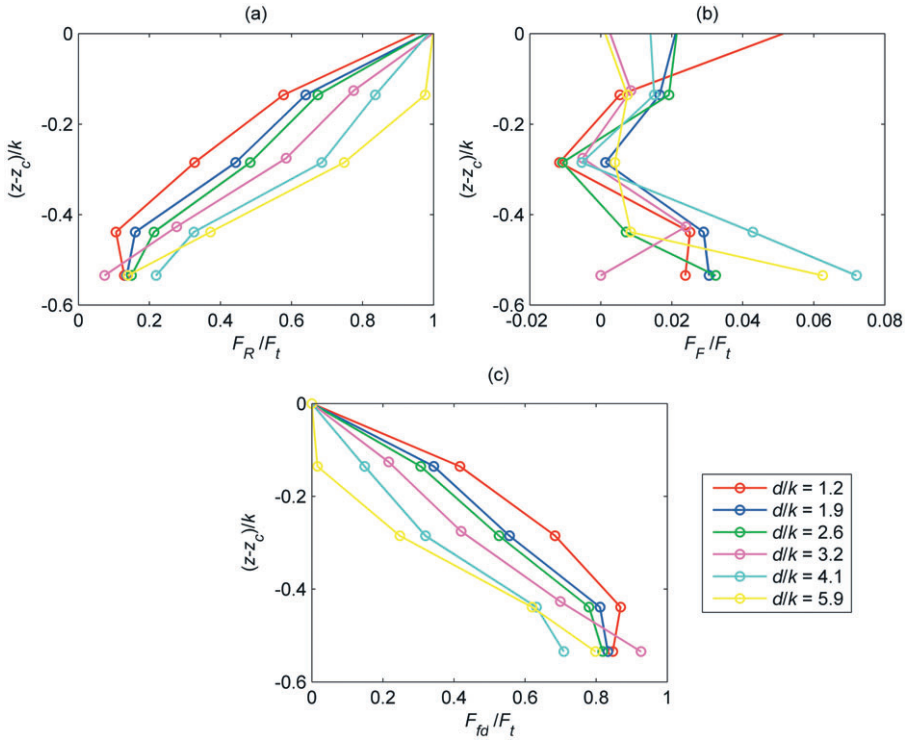

Figure 3. Vertical distribution of force components within the roughness elements over a defined plan area A_0 for a range of relative submergences over the unimodal deposit. This figure is available in colour online at www.interscience.wiley.com/journal/espl

turbulent momentum exchange across the fluid–boundary interface (Zhou and Mendoza, 1993; Packman *et al.*, 2004). Furthermore it has been observed that the magnitude of hyporheic exchange increases with Reynolds number (Packman *et al.*, 2004), and therefore also rises with relative submergence at a single bed slope. Figure 3 displays fluid measurements which provide physical evidence for this observation.

The reduction in force from Reynolds stress is accompanied by an increase in the contributions from form drag as the flow becomes shallower. This corresponds with observations that shallower flows are more roughness dominated and exhibit a greater relative reduction in Reynolds stress than flows that are several times the depth of the height of the roughness elements. Figure 3 also reveals that the contributions from form-induced stress display some tendency to be higher for the larger submergences, especially in the lower parts of the roughness layer. This indicates that, even with the same bed surface topography, momentum transfer mechanisms and sediment–water interface exchange processes will change with an increase in relative submergence.

A comparison is made in Figure 4 of the relative contributions of the force components over the two water-worked sediment deposits. It reveals that the differences between the two deposits change according to height within the roughness layer. At similar levels of relative submergence and at the same vertical position within the upper ~25% of the roughness layer, the force contributions caused by turbulence are lower over the unimodal deposit. Also within this upper 25%, form drag has a much greater influence on the force experienced by grains within the surface layer of this deposit. In contrast, within the lower ~75% of the roughness layer, the contributions from Reynolds stress are lower over the bimodal deposit, but greater from form drag at similar levels of relative submergence. Within this lower 75%, form-induced force tends to have a different vertical distribution over both deposits in that the force direction is different. These results highlight that the momentum transfer mechanisms differ over the two deposits at the same levels of relative submergence. The vertical subdivision in differences between the two deposits closely resembles the differences in surface geometry and porosity (Figure 1). This reveals that for deposits with different geometries and lower porosities, such as gravel–sand deposits, the drag force component of the total force is higher and the temporally variable fluid shear stress component is lower at the bed surface interface. This pattern coincides with the observations of Packman *et al.* (2006) who found that the hyporheic exchange with a gravel-sand bed, thought to be caused by turbulent momentum exchange, was much slower than for a gravel bed.

A number of flume experiments have revealed that a greater supply or presence of sand will tend to increase the total transport rate within a river channel. They have shown that this is caused by a rise in the transport capacity of not only the sand, but also the gravel fractions in the river bed (Jackson and Beschta, 1984; Ikeda and Iseya, 1988; Wilcock *et al.*, 2001; Curran and Wilcock, 2005; Curran, 2007). It was concluded that this increase is too large to be attributed purely to a decrease in the surface grain size. This would suggest that other factors must be responsible for their observed rise in total sediment transport due to the presence of sand on the surface. The difference in the force contributions between the unimodal and bimodal deposits may provide a possible explanation. It has been demonstrated by others that some aspect of streamwise velocity strongly correlates with sediment entrainment transport, but that the cross products of velocity have a poorer relationship with sediment entrainment (Williams *et al.*, 1989; Nelson *et al.*, 1995; Papanicolaou *et al.*, 2001; Schmeeckle and Nelson, 2003). For example, Bottacin-Busolin *et al.* (2008) discovered that over half of the grain movements observed over a gravel bed were due to variations in the streamwise component of velocity, and only in a relatively small percentage of the cases (around one-tenth) were they characterised by changes in the cross-product of temporal fluctuations in velocity. In simple terms, entrainment appears

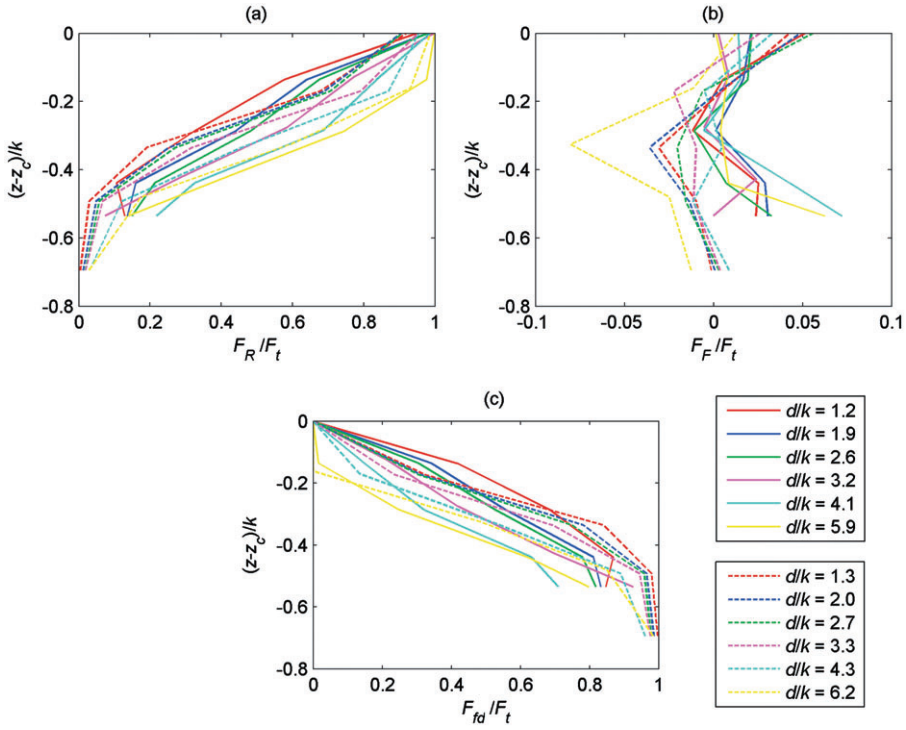

Figure 4. Vertical distribution of force components within the roughness elements over a defined plan area A_0 for the two water-worked gravel deposits. Solid lines denote the unimodal deposit and dashed lines denote the bimodal deposit. This figure is available in colour online at www.interscience.wiley.com/journal/espl

to correlate well with form drag but not so well with temporally variable fluid shear stress. Given that the results in Figure 4 suggest that in gravel–sand deposits the drag force component of the total force is higher for similar flow conditions (bed slope and relative submergence) and D_{50}, it could explain why they exhibit greater mobility relative to deposits which contain purely gravel.

If the measurements of each of the force components in Figure 4 were extrapolated down to the roughness trough, the force from Reynolds and form-induced stress would continue to decrease because a higher proportion of the total force would be extracted by the form drag associated with bed surface grains or bedforms. For both deposits, at the roughness trough, the force from Reynolds stress is likely to diminish completely. This might occur at a higher elevation for the bimodal deposit and could be caused by exhibiting a lower porosity within the roughness layer and the subsurface. The experimental results would appear to support the hypothesis of Manes *et al.* (2007) that the spatially-averaged force at the roughness trough is entirely composed of the fluid drag on all the roughness elements. This would represent the contribution to the total resisting force caused by the interaction of the surface and subsurface flow in the porous deposit, and would suggest that fluid momentum flux between the bed surface and subsurface is negligible.

Conclusions

The analysis presented in this commentary has shown that if co-located, high quality spatial data on the flow velocity and bed surface topography data is obtained then it is possible to decompose the total fluid force on a water-worked bed into meaningful physical components. These components represent the contribution of form drag, turbulence and spatial flow variation, and are derived from the double-averaged Navier–Stokes momentum equations.

The relative size of each of these components was determined using data collected from different water-worked gravel deposits. One deposit was created from a unimodal gravel mixture and the other from a bimodal, gravel–sand mixture. The deposits had a similar median grain size but different vertical distributions of bed surface elevations (roughness geometries) and deposit porosity. By analysing the flow velocity data using an approach based on temporal and spatial averaging, and assessing drag using the topography data, it was possible to determine the vertical variation in forces caused by form drag, turbulence and flow spatial heterogeneity. The pattern of these variations indicated that relative submergence, surface geometry and possibly deposit porosity all had an impact on the relative size of these components.

It was shown that drag generated forces were higher at lower submergences over both deposits. In the gravel surface layer there was a wider variation in turbulence generated forces than for the gravel–sand deposit. The form-induced forces were generally smaller, but the pattern was significantly different over the two deposits, especially deep within the bed roughness layer. The variation in drag generated forces between the two deposits and with different flow submergences is likely to influence grain entrainment. The lower values of turbulence generated and form-induced forces in the gravel–sand deposit may indicate an impact on the ability to transfer momentum at the sediment–water interface. This would impact on fluid driven bed processes, such as the exchange of soluble and fine particulate pollutants between the overlying flow and the pore water within the deposit.

The work in the paper enables the boundary shear stress to be linked explicitly to surface roughness properties and therefore the approach has the potential to be used for the upscaling of the impact of boundaries in spatially variable, turbulent

flows. By considering the physical components of shear stress and their relative sizes it is possible to provide physically based explanations of existing observations of enhanced mobility of gravel–sand mixtures and the transfer of solutes into porous, sediment deposits.

References

Bottacin-Busolin A, Tait SJ, Marion A, Chegini A, Tregnaghi M. 2008. Probabilistic description of grain resistance from simultaneous flow field and grain motion measurements. *Water Resources Research* **44**: DOI:10·1029/2007WR006224.

Campbell L, McEwan I, Nikora V, Pokrajac D, Gallagher M, Manes C. 2005. Bed-load effects on hydrodynamics of rough-bed open-channel flows. *Journal of Hydraulic Engineering, ASCE* **131**: 576–585.

Cooper JR. 2006. Spatially-induced momentum transfer over water-worked gravel beds. PhD thesis, University of Sheffield, Sheffield, UK.

Cooper JR, Tait SJ. 2008. The spatial organisation of time-averaged streamwise velocity and its correlation with the surface topography of water-worked gravel beds. *Acta Geophysica* **56**: 614–641.

Cooper JR, Tait SJ. 2009. Water-worked gravel beds in laboratory flumes – a natural analogue? *Earth Surface Processes and Landforms* **34**: 384–397.

Curran JC. 2007. The decrease in shear stress and increase in transport rates subsequent to an increase in sand supply to a gravel-bed channel. *Sedimentary Geology* **202**: 572–580.

Curran JC, Wilcock PR. 2005. Effect of sand supply on transport rates in a gravel-bed channel. *Journal of Hydraulic Engineering, ASCE* **131**: 961–967.

Hardy RJ, Best JL, Lane SN, Carbonneau PE. 2009. Coherent flow structures in a depth-limited flow over a gravel surface: the role of near-bed turbulence and influence of Reynolds number. *Journal of Geophysical Research* **114**: DOI:10·1029/2007JF000970.

Ikeda H, Iseya F. 1988. Experimental study of heterogeneous sediment transport. Paper 12, Environment Research Centre, University of Tsukuba, Tsukuba, Japan.

Jackson WL, Beschta RL. 1984. Influences of increased sand delivery on the morphology of sand and gravel channels. *Water Resources Bulletin* **20**: 527–533.

Lamarre H, Roy AG. 2005. Reach scale variability of turbulent flow characteristics in a gravel-bed river. *Geomorphology* **68**: 95–113.

Manes C, Pokrajac D, McEwan I. 2007. Double-averaged open-channel flows with small relative submergence. *Journal of Hydraulic Engineering, ASCE* **133**: 896–904.

Nelson JM, Shreve RL, Mclean SR, Drake TG. 1995. Role of near-bed turbulence structure in bed-load transport and bed form mechanics. *Water Resources Research* **31**: 2071–2086.

Nikora V, Goring D. 2000. Flow turbulence over fixed and weakly mobile gravel beds. *Journal of Hydraulic Engineering, ASCE* **126**: 679–690.

Nikora V, McEwan I, McLean S, Coleman S, Pokrajac D, Walters R. 2007. Double-averaging concept for rough-bed open-channel and overland flows: theoretical background. *Journal of Hydraulic Engineering, ASCE* **133**: 873–883.

Packman AI, Zaramella M, Chen C, Gaillard J, Keane DT. 2006. Development of layered sediment structure and its effects on pore water transport and hyporheic exchange. *Water, Air and Soil Pollution: Focus* **6**: 69-78.

Packman A, Salehin M, Zaramella M. 2004. Hyporheic exchange with gravel beds: basic hydrodynamic interactions and bedform-induced advective flows. *Journal of Hydraulic Engineering, ASCE* **130**: 647–656.

Papanicolaou AN, Diplas P, Dancey CL, Balakrishnan M. 2001. Surface roughness effects in near-bed turbulence: implications to sediment entrainment. *Journal of Engineering Mechanics, ASCE* **127**: 211–218.

Roy AG, Buffin-Bélanger T, Lamarre H, Kirkbride AD. 2004. Size, shape and dynamics of large-scale turbulent flow structures in a gravel-bed river. *Journal of Fluid Mechanics* **500**: 1–27.

Schmeeckle MW, Nelson JM. 2003. Direct numerical simulation of bedload transport using a local, dynamic boundary condition. *Sedimentology* **50**: 279–301.

Schmeeckle MW, Nelson JM, Shreve RL. 2007. Forces on stationary particles in near-bed turbulent flows. *Journal of Geophysical Research* **112**: DOI:10.1029/2006JF000536.

Shvidchenko AB, Pender G. 2001. Macroturbulent structure of open-channel flow over gravel beds. *Water Resources Research* **37**: 709–719.

Wilcock PR, Kenworthy ST, Crowe JC. 2001. Experimental study of the transport of mixed sand and gravel. *Water Resources Research* **37**: 3349–3358.

Williams JJ, Thorne PD, Heathershaw AD. 1989. Measurements of turbulence in the benthic boundary-layer over a gravel bed. *Sedimentology* **36**: 959–971.

Zhou DH, Mendoza C. 1993. Flow through porous bed of turbulent stream. *Journal of Engineering Mechanics, ASCE* **119**: 365–383.